In Vitro Pulsatility Analysis of Axial-Flow and Centrifugal-Flow Left Ventricular Assist Devices

J. Ryan Stanfield
Department of Mechanical Engineering,
University of Utah,
50 S Central Campus Dr.,
Rm. 2110, Salt Lake City, UT 84112
e-mail: ryan.stanfield@utah.edu

Craig H. Selzman
Department of Surgery,
Division of Cardiothoracic Surgery,
University of Utah,
30 N 1900 E, SOM 3C127,
Salt Lake City, UT 84132

Recently, continuous-flow ventricular assist devices (CF-VADs) have supplanted older, pulsatile-flow pumps, for treating patients with advanced heart failure. Despite the excellent results of the newer generation devices, the effects of long-term loss of pulsatility remain unknown. The aim of this study is to compare the ability of both axial and centrifugal continuous-flow pumps to intrinsically modify pulsatility when placed under physiologically diverse conditions. Four VADs, two axial- and two centrifugal-flow, were evaluated on a mock circulatory flow system. Each VAD was operated at a constant impeller speed over three hypothetical cardiac conditions: normo-tensive, hypertensive, and hypotensive. Pulsatility index (PI) was compared for each device under each condition. Centrifugal-flow devices had a higher PI than that of axial-flow pumps. Under normo-tension, flow PI was 0.98 ± 0.03 *and* 1.50 ± 0.02 *for the axial and centrifugal groups, respectively* ($p < 0.01$). *Under hypertension, flow PI was* 1.90 ± 0.16 *and* 4.21 ± 0.29 *for the axial and centrifugal pumps, respectively* ($p = 0.01$). *Under hypotension, PI was* 0.73 ± 0.02 *and* 0.78 ± 0.02 *for the axial and centrifugal groups, respectively* ($p = 0.13$). *All tested CF-VADs were capable of maintaining some pulsatile-flow when connected in parallel with our mock ventricle. We conclude that centrifugal-flow devices outperform the axial pumps from the basis of PI under tested conditions.* [DOI: 10.1115/1.4023525]

Keywords: left ventricular assist device, mechanical circulatory support, axial flow blood pump, centrifugal flow blood pump, pulsatility

1 Introduction

Mechanical circulatory support is an important and increasingly prevalent therapy for patients with advanced heart failure. Ventricular assist devices (VADs) are broadly distinguished as either volume-displacement (pulsatile-) or continuous-flow pumps. The advantages and disadvantages of pulsatile versus nonpulsatile blood flow have been chronicled and deliberated for decades [1,2]. However, the acceptance and increasing use of continuous-flow systems has come about by ongoing research demonstrating excellent recovery of failing end-organs and enhanced survival [3–5]. Rotary VADs have alleviated several concerns that earlier volume-displacement pumps experienced, including efficiency [6], anatomic fit [7], durability [8], hemolysis [9], and reliability [10]. Physically, the continuous-flow pumps have traded in a decrease in pulse pressure for a smaller sized device. With the lasting effects of chronic nonpulsatile flow unknown and the widespread and increasing use of these devices, examination of VAD responses to inherent fluctuations in preload and afterload and performance during moderate pulsatile-flow is clinically relevant.

As the designs of CF-VADs continue to evolve, maintaining or producing pulsatile-flow is a sought-after positive feature. Quantifying the level of pulsatile-flow through a CF-VAD establishes a metric by which different devices can be compared. Pulsatility index (PI) is defined as a measurement for variability of the fluid flow rate. PI is calculated to relate devices to the level of pulsatile flow that is generated under a given condition. Some CF-VADs report PI on the system monitor and use it for speed control [11,12]. Even if PI is not reported, an estimated flow rate usually is, so it is possible to estimate PI as the amplitude in flow rate varies.

We have observed clinically that various CF-VADs are capable of greater PI than others. To date, however, no reports exist that experimentally contrast multiple continuous-flow devices under pulsating-type, hence physiologic, conditions. Comparison of implanted devices involves too many variables for direct scientific analysis and if attempted would require a very large sample group to be statistically viable. A mock flow loop provides greater control over the parameters in the circulation than the *in vivo* situation. *In vitro* experiments designed to analyze VAD performance under pulsating pressure and flow will show how they compare to one another under physiologic conditions. Clinically, we are faced with real, important challenges in patient management based on both the loading (volume status) and unloading (hypertension) conditions of the ventricle. In this study we investigate the variations in *in vitro* pulsatility characteristics generated by four CF-VADs, two axial-flow type and two centrifugal- (or radial-) flow design.

2 Materials and Methods

The mock circulation system (Fig. 1) consists of atrium (LA), ventricle (LV), and lumped systemic (SCC) and pulmonary (PCC) compliance/resistance chambers, similar to that described by Pantalos, et al. [13], hybridized with our open-loop flow system described elsewhere [14]. Both artificial atrium and ventricle are made of flexible polyurethane sacs, with the ventricular sac housed in a pressurization chamber. The ventricle top supports mounting for inflow (mitral) and outflow (aortic) prosthetic

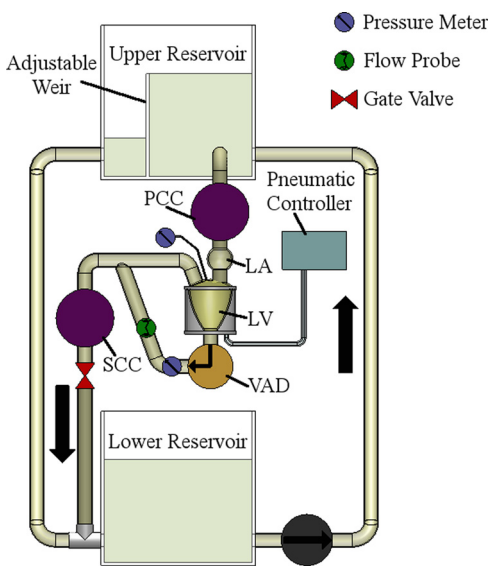

Fig. 1 Schematic of mock circulation loop with pulsatile capability. PCC/SCC, pulmonary/systemic compliance chamber(s); LA, left atrium; LV, left ventricle. Not shown: unidirectional pericardial valves at "top" of LV to represent mitral and aortic valves.

Contributed by the Bioengineering Division of ASME for publication in the Journal of Biomechanical Engineering. Manuscript received October 6, 2012; final manuscript received January 21, 2013; accepted manuscript posted January 29, 2013; published online February 11, 2013. Assoc. Editor: Ender A. Finol.

Table 1 Cardiac conditions for pulsatile flow analysis. LVP, left ventricular pressure (mm Hg); LAP, left atrial pressure (mm Hg); MAP, mean arterial pressure (mm Hg); Q_{AV}, average flow rate through aortic valve (L/min)

Condition	Model	LVP	LAP	MAP	Q_{AV}
1	Normo-tensive	110	15	90	0.5
2	Hypertensive	150	15	120	0.4
3	Hypotensive	80	5	60	0.3

valves. Porcine pericardial valves (Baxter, Deerfield, IL) are employed for this experiment. Contraction and pulsatile-flow is sustained by connection of the ventricular chamber to a pneumatic controller. Additionally, the loop employs reservoirs filled with a blood-analog fluid (~40% glycerin in water at 36 °C; Hi-Valley Chemical, Centerville, UT) with a dynamic viscosity of 3.6 cP. All connections between chambers and reservoirs are made using Tygon® tubing (Saint-Gobain, Courbevoie, France). A manual gate valve was placed after the SCC to adjust the resistance (afterload). All items shown between the upper and lower reservoirs were maintained on the same horizontal plane to minimize compounding effects of gravity but are illustrated in the figure in a vertical orientation for convenience.

With the mock circulation loop capable of pulsatile pressure and flow, VADs are tested by simulated LV apex cannulation and aortic anastomosis. The four VADs under analysis are the HeartMate II (Thoratec Corp., Pleasanton, CA), the Jarvik 2000 (Jarvik Heart Inc., New York, NY), the Levacor (WorldHeart Corp., Salt Lake City, UT), and the VentrAssist (Ventracor Ltd., Sydney, Australia), which are referred to as axial 1 (A1), axial 2 (A2), centrifugal 1 (C1), and centrifugal 2 (C2), respectively. Investigation is carried out on each device under three pulsatile conditions: normo-tensive, hypertensive, and hypotensive. Pressure values significant and adjustable to each cardiac condition are displayed in Table 1. All three conditions maintain a uniform beat rate of 100 beats per minute (bpm) and a stiff systemic compliance of 0.5 mL/mm Hg. Outflow rate from the ventricle via the aortic valve (Q_{AV}) is also contained in Table 1, where no significant difference was seen between devices.

Table 2 Impeller radius and inlet area for each device. *A*, inlet area (mm²); *R*, impeller radius (mm)

	Axial 1 (A1)	Axial 2 (A2)	Centrifugal 1 (C1)	Centrifugal 2 (C2)
A	113	104	113	79
R	6	7	25	20

The pump flow rate (Q) was measured with an ultrasonic flow meter and flow probe (Transonic, Ithaca, NY). Pump preload, or inflow pressure (P_i), and pump afterload, or outflow pressure (P_o), are measured with fluid-filled transducers (Edwards LifeSciences, Irvine, CA) and a pressure meter (Living Systems Instrumentation, St. Albans, VT). Acquisition of flow meter and pressure meter data signals was performed at 40 Hz with a custom system (National Instruments, Austin, TX). For data analysis and plotting, MATLAB (v6.5; MathWorks, Natick, MA) and a spreadsheet program (Excel 2007, Microsoft, Redmond, WA) were used.

Each analysis is done at a single impeller speed for each pump. Because of the inherent differences between axial- and centrifugal-flow pumps, running all four devices at the same speed (rpm) is not feasible for allowing suitable comparisons. Thus, we selected speeds for each pump that we have previously used as determined by

Table 3 Flow rate, pressure differential, flow and head coefficients, and pulsatility results for axial- and centrifugal-flow devices under the pulsatile cardiac models. *Q*, flow rate (L/min); ΔP, pressure differential (mm Hg); φ, flow coefficient; ψ, head coefficient; PI_Q, flow pulsatility index; R_{pul}, pulsatility ratio. One-way ANOVA was used for *Q*, ΔP, φ, and ψ across both devices and conditions, with *p*-values for column data in the last two rows.

Condition	Metric	Axial 1 (A1)	Axial 2 (A2)	Centrifugal 1 (C1)	Centrifugal 2 (C2)
Speed		9000	10,000	2000	2000
Normo-tensive	$Q \pm$ SD	4.8 ± 1.6	3.9 ± 1.4	3.5 ± 2.0	3.8 ± 2.0
	$\Delta P \pm$ SD	55 ± 24	66 ± 28	68 ± 24	64 ± 29
	$\phi \pm$ SD ($p < 0.001$)	0.13 ± 0.04	0.09 ± 0.03	0.10 ± 0.06	0.19 ± 0.10[a]
	$\psi \pm$ SD ($p < 0.001$)	0.22 ± 0.10	0.17 ± 0.07	0.29 ± 0.11[a]	0.43 ± 0.19[a]
	PI_Q	0.96	1.00	1.49	1.51
	R_{pul}	0.56	0.80	1.40	1.04
Hypertensive	$Q \pm$ SD	3.4 ± 2.5[b]	3.1 ± 2.1	1.9 ± 3.1[b]	2.2 ± 3.2[b]
	$\Delta P \pm$ SD	70 ± 38	81 ± 40	82 ± 32[b]	73 ± 41
	$\phi \pm$ SD	0.09 ± 0.07[b]	0.07 ± 0.05	0.05 ± 0.09[b]	0.11 ± 0.16[b]
	$\psi \pm$ SD ($p < 0.001$)	0.28 ± 0.15	0.20 ± 0.10[a]	0.35 ± 0.14[b]	0.49 ± 0.28[a]
	PI_Q	2.01	1.79	4.41	4.01
	R_{pul}	1.03	1.25	3.96	2.17
Hypotensive	$Q \pm$ SD ($p < 0.001$)	5.0 ± 1.3	3.4 ± 0.9[a]	4.5 ± 1.3	4.6 ± 1.3
	$\Delta P \pm$ SD ($p < 0.05$)	53 ± 19	47 ± 23[ab]	59 ± 18	63 ± 21
	$\phi \pm$ SD ($p < 0.001$)	0.14 ± 0.04	0.08 ± 0.02[a]	0.13 ± 0.04	0.23 ± 0.07[a]
	$\psi \pm$ SD ($p < 0.001$)	0.21 ± 0.08	0.12 ± 0.06[a,b]	0.25 ± 0.08	0.43 ± 0.14[a]
	PI_Q	0.74	0.72	0.76	0.80
	R_{pul}	0.54	0.47	0.81	0.73
All	Q (ϕ)	$p < 0.01$	$p < 0.21$	$p < 0.002$	$p = 0.002$
	ΔP (ψ)	$p < 0.09$	$p < 0.004$	$p < 0.02$	$p < 0.53$

[a]Indicates significant difference across row (single condition).
[b]Indicates significant difference among column (single device).

comparison of pressure-flow performance curves, as well as clinical experience [15]. Speeds selected for A1, A2, C1, and C2 pumps were 9000, 10,000, 2000, and 2000 rpm, respectively. Tests were repeated three times in order to account for variability in the system.

2.1 Calculations. A portion of the captured data yields a set of points showing the variability of flow rate over time. The data will be used to calculate pulsatility index for flow (PI_Q), which is the difference between maximum and minimum flow rates divided by the average flow rate, or Eq. (1). Choi, et al. described another useful pulsatility metric as the pulsatility ratio [16,17]. The pulsatility ratio (R_{pul}) is a ratio of pulsatility indices for flow and pressure ($R_{pul} = PI_Q/PI_{\Delta P}$). For this the preload and afterload data points were used to compute a pressure differential waveform against time. From the pressure differential waveform, a pulsatility index for pressure differential ($PI_{\Delta P}$) will be computed via Eq. (2). The calculations described here will be used to assess the level of pulsatile-flow that the analyzed continuous-flow devices are able to generate while connected in parallel with a synthetic heart.

$$PI_Q = \frac{Q_{max} - Q_{min}}{Q_{avg}} \tag{1}$$

$$PI_{\Delta P} = \frac{\Delta P_{max} - \Delta P_{min}}{\Delta P_{avg}} \tag{2}$$

Flow rate and pressure data are compared using the dimensionless coefficients for flow (φ) and head (ψ) [18], defined by Eqs. (3) and (4), where A is the area of inlet or outlet (m^2), R is the radius of impeller (m), Ω is rotational speed of the impeller (rad/s), g is acceleration due to gravity (m/s^2), and H is head (Pa). Relevant dimensions for coefficient calculation are presented in Table 2.

$$\varphi = \frac{Q}{AR\Omega} \tag{3}$$

$$\psi = \frac{gH}{R^2\Omega^2} \tag{4}$$

Continuous flow rate, pressure differential, flow coefficient, and head coefficient data are presented as mean ± SD (Table 3). Percentages are used for categorical data. Results were compared by t-test or by one-way analysis of variance. Statistical significance was considered at $p < 0.05$.

3 Results

We first sought to create a physiologic *in vitro* model system that allows for the dynamic, rather than static, testing of the axial- and centrifugal-flow devices. Figure 2 graphically depicts three clinically relevant baseline conditions: normo-tensive, hypertensive, and hypotensive. As demonstrated, the peak systolic left ventricular pressure (LVP) exceeds the nominal aortic pressure (*AoP*) signifying that the aortic valve (AV) continues to open for all three conditions. Opening of the AV during VAD implantation may also be referred to as partial-support, as opposed to full-support, where the AV does not open. The first condition, normo-tensive, was selected as a partial-support baseline. The second and third conditions are high and low variations, respectively, for relative pressures. As expected, the hypertensive case shows the largest diastolic pressure differentials of the three, with the hypotensive case showing the smallest. All four pumps were subjected to each of the three pulsatile cardiac conditions on the mock circulation loop.

The pulsatile, dimensionless coefficient waveforms φ and ψ calculated for each device under all conditions on the mock loop are shown in Fig. 3. The waveforms are displayed over a brief 3 s window during the operation of each device. With all devices the peak in φ coincides closely with the dip in ψ. Thus, highest flow occurs during systole when the AV is open and the transaortic pressure gradient is minimal. Data from the waveforms are used to compute pulsatility characteristics, which are presented in Table 3.

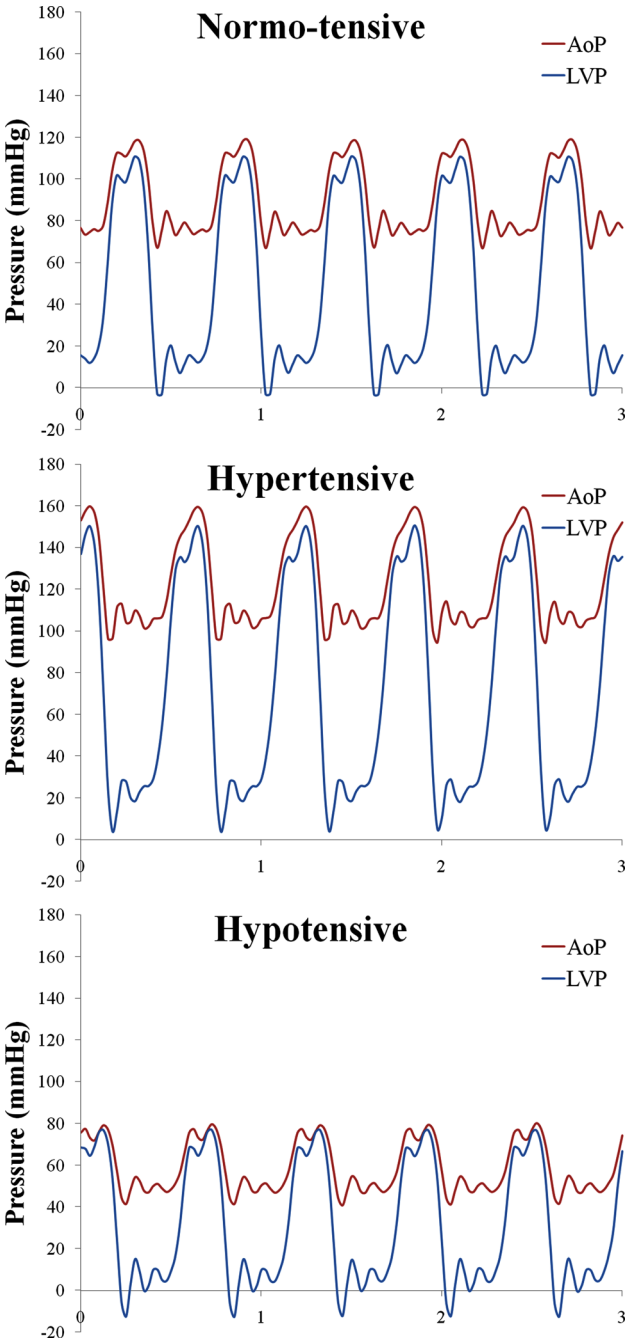

Fig. 2 Baseline oscillating pressure waveforms associated with each simulated cardiac condition: normo-tensive, hypertensive, and hypotensive. AoP, aortic pressure; LVP, left ventricular pressure (mm Hg).

Under the normo-tensive condition, (first column in Fig. 3), the average Q for axial devices is slightly greater (16%) than centrifugal ones; however, the PI_Q and R_{pul} are much greater for centrifugal devices, as are the flow and head coefficients, φ and ψ. PI_Q was 0.98 ± 0.03 and 1.50 ± 0.02 for the axial and centrifugal groups, respectively ($p < 0.01$). Similarly, the second and third columns in Fig. 3 show pulsatile φ and ψ waveforms for each pump under the hypertensive and hypotensive models, respectively. A point of interest under the hypertensive case shows that both centrifugal devices experience negative, or reverse, flow, also known as pump regurgitation. Negative flow can have a significant impact on the physiological system, as well as on computation of *PI*. PI_Q and R_{pul} of centrifugal devices under hypertension is double that of the axial

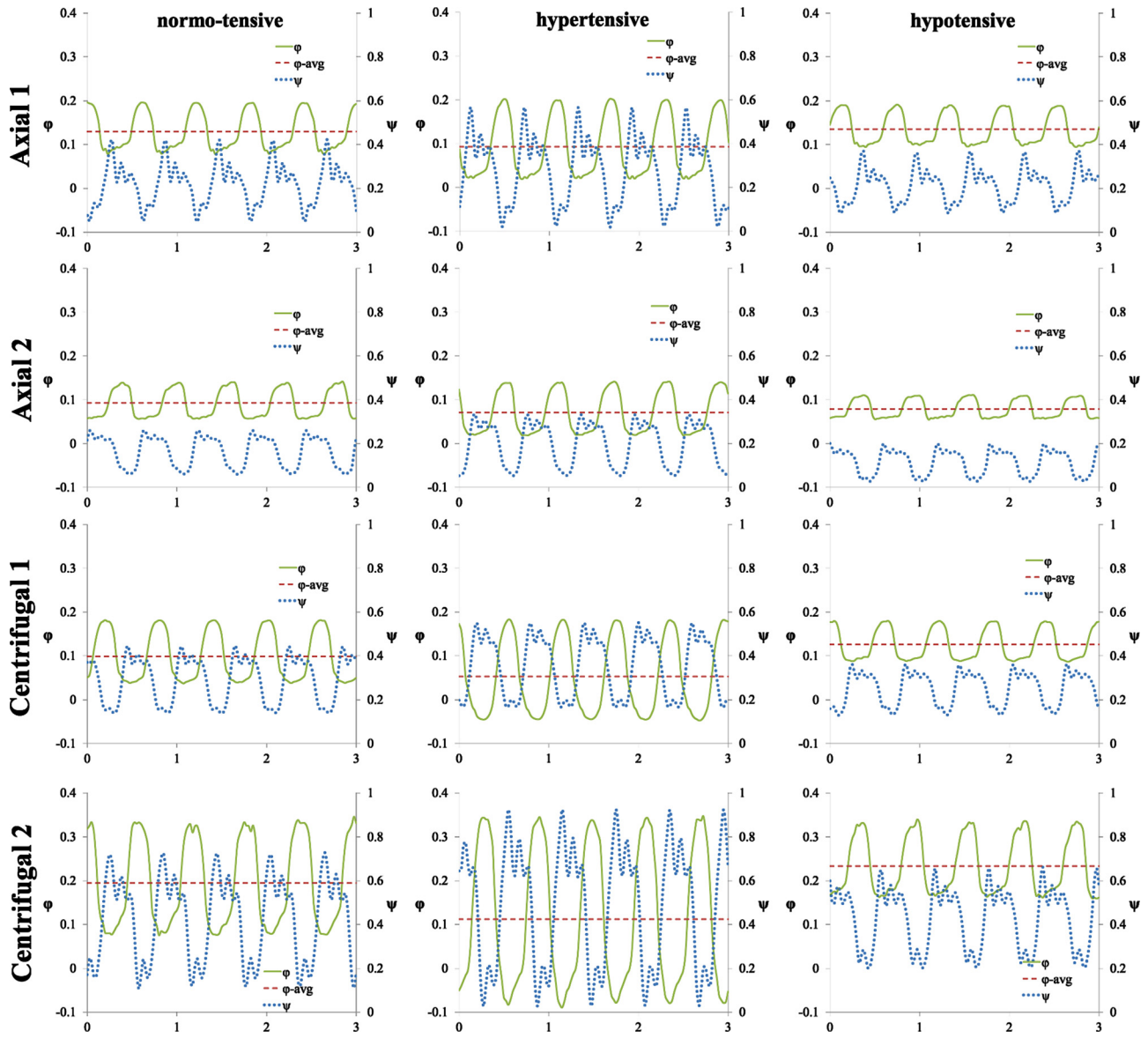

Fig. 3 Oscillating head and flow coefficient waveforms under all tested conditions for axial (A1, A2) and centrifugal (C1, C2) continuous-flow pumps. φ, flow coefficient; ψ, head coefficient. Left column are waveforms for all pumps under normo-tensive condition, middle column under hypertensive condition, right column under hypotensive condition.

pumps. PI_Q was 1.90 ± 0.16 and 4.21 ± 0.29 for the axial and centrifugal groups, respectively ($p = 0.01$).

No statistical significance was seen when comparing the Q or ΔP under normo-tensive or hypertensive conditions, but after normalization there were significant differences in ψ under these conditions. Additionally, hypotension shows variation in mean Q and ΔP for A2 (further illustrated in Fig. 4), as well as φ and ψ. The similarity between Q and ΔP yields PI_Q that is nearly uniform between the pumps: 0.73 ± 0.02 and 0.78 ± 0.02 for the axial and centrifugal groups, respectively ($p = 0.13$). Interestingly, R_{pul} for the centrifugal devices remain above those yielded by axial-flow pumps. R_{pul} was 0.50 ± 0.05 and 0.77 ± 0.06 for the axial and centrifugal groups, respectively ($p < 0.04$).

Figure 4 presents the pressure-flow—both ΔP versus Q and ψ versus φ-relationship for each device under all three simulated cardiac conditions. The pressure-flow performance curve, or dynamic characteristic curve, for each device follows a clockwise loop, with systole covering the right and lower portions of the loop and diastole over the left and upper sections. The size of a performance loop is directly related to the amount of hydraulic power supplied by each device. Hydraulic power, calculated by integrating the area within the performance loops, is displayed in Fig. 5. All devices show distinctively greater power in hypertension and lower power in hypotension. A1 is markedly lower than the other three devices in all conditions, except for C1 under hypertension. However, power differences between the groups (axial versus centrifugal) are not statistically significant.

4 Discussion

The common goal of all VADs is to augment systemic cardiac output and reduce the load on the ventricle during the cardiac cycle without leading to significant biological or hematological complications. Accomplishing this goal while maintaining evolutionarily preserved physiology, i.e., pulsatility, may influence the ability of these devices to provide beneficial and durable support for the advanced heart failure patient. Comparative efficacy of pulsatile- and continuous-flow VADs have extensively documented their effects on ventricular unloading [19,20], hemodynamics [21,22], end organ function, and microcirculation [23], as well as vascular reactivity [24]. While continuous-flow devices are not pulsatile by design, we show that some designs exhibit greater induced pulsatility than others.

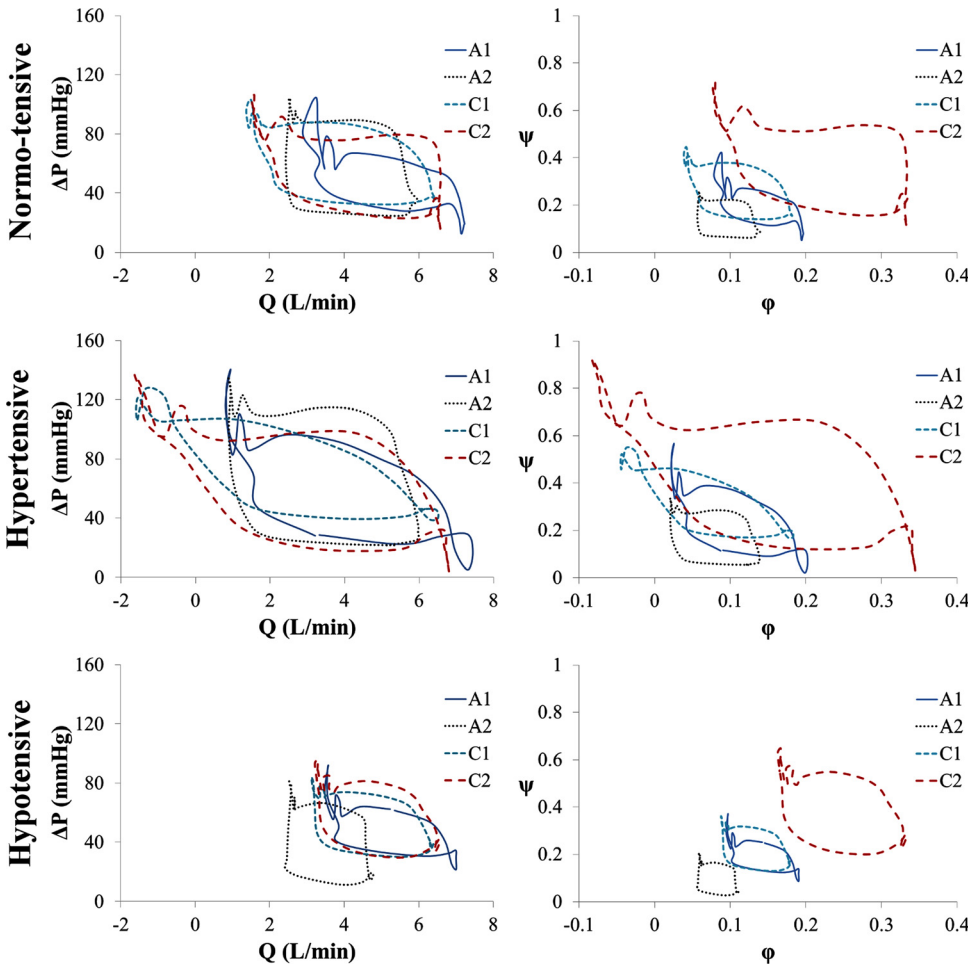

Fig. 4 Pressure-flow (first column: ΔP-Q; second column: ψ-φ) performance curves for all four devices under the three tested conditions. Q, flow rate (L/min); ΔP, pressure differential (mm Hg); φ, flow coefficient; ψ, head coefficient.

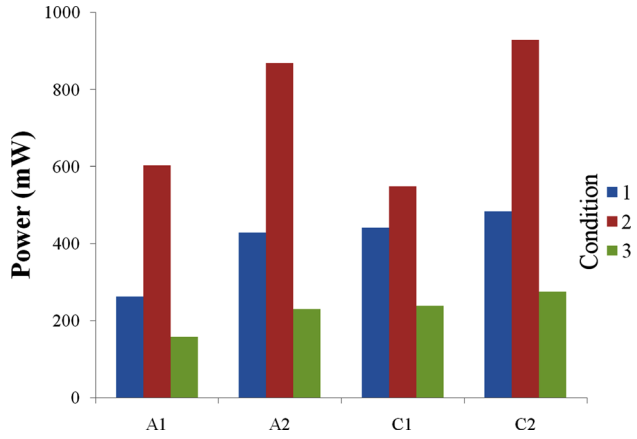

Fig. 5 Hydraulic power (mW), supplied by each VAD in a typical cycle under the pulsatile cardiac conditions: (1) normotensive, (2) hypertensive, and (3) hypotensive

Our study compares pulsatility characteristics of two axial-flow and two centrifugal-flow VADs under varying physiologic conditions. We show the centrifugal-flow device design to produce greater pulsatile flow than the axial-flow device, when connected in parallel with a synthetic, pulsating ventricle. The difference is most notable under low-flow, high-pressure circumstances, which agrees with typical design environment settings for centrifugal-flow pumps [18].

We further show that pulsatility ratio is higher in the centrifugal rather than the axial-flow devices. Choi, et al. show that ventricular suction events occur with a decrease in R_{pul} and state that it is a more reliable metric to mitigate suction events than is the PI_Q metric [16]. We postulate that R_{pul} can be employed as a qualitative metric to predict which device design will be more or less prone to alleviate suction events. Ultimately, suction events are a function of patient anatomy, physiological condition, inflow orientation, and more. However, R_{pul} should be considered as a viable metric that may abate the occurrence of such events.

The influence of VAD therapy on positive cardiac remodeling and improvement in LV function remains an active, and often disputed, field of investigation [25,26]. It is unknown to what extent the differences observed in $\underline{PI}_Q$ between the axial-flow pumps and centrifugal-flow pumps have on the potential for LV recovery. Recovery is thought to be associated with unloading the LV. However, long-term full-support, or complete unloading, where the aortic valve ceases to open during the cardiac cycle, may lead to muscle atrophy. Our study does not consider the full-support case, to which many VAD recipients are subject immediately after implantation. This study only considers partial-support for all analyzed cardiac conditions, which may be preferred for long-term support. More volume unloading could have been achieved by increased impeller speed in each device; however, speeds common to current clinical implementation were employed. Limitation in this study is also due to the Newtonian fluid used as a blood-analog, where the implementation of a non-Newtonian fluid may have further insight into pump performance and variability.

The ΔP-Q performance loop illustrates the considerable distinction between systole and diastole that a pump experiences during implantation. Typical *in vitro* analysis, under continuous-flow conditions, yields pressure-flow performance to be a single curve for a given impeller speed [27]. However, we show that the clinical application of the continuous-flow rotary pump connected in parallel with a pulsing system yields a noticeably altered performance curve, or in this case, performance loop. This illustrates the dynamic environment to which the VAD is subject. End-diastole to early-systole appears to be similar to steady-state hydrodynamic performance curves in most cases, but end-systole to early-diastole is divergent. With LVP alternately increasing and decreasing throughout the cardiac cycle, the output variable(s) (Q, AoP) form a rate-dependent hysteresis loop. The hysteresis loop occurs due to the relative sinusoidal waveform oscillations of pressure and flow (ψ and φ) being out of phase with one another: That is, ΔP (ψ) increases while Q (φ) decreases, and vice versa, which is due to overall dynamic lag in the system. The lag is due, in part, to the compliant nature of the various chambers throughout the experimental test loop. The phase imbalance is also due to the design of each pump system, primarily the speed tolerance within the motor controller. We expect analogous alteration of pressure and flow to be present in the implanted configuration. Similar to the ΔP-Q loop, the dimensionless ψ-φ performance loop illustrates the difference in design between the four devices, where some ψ-φ instances do overlap each other, but the average head and flow coefficients are markedly different due to fundamental hydraulic design variations [14].

5 Conclusion

In conclusion, our study indicates that both axial and centrifugal continuous-flow pump designs maintain some pulsatile flow when connected in parallel with the ventricle. Of the two designs, the centrifugal-flow provides significantly greater pulsatility index when exposed to physiologic conditions of varying preload and afterload. Further, the pulsatility ratio exhibited by the centrifugal-flow designs lead us to believe that they are more likely to abate suction events. Improved response to changes in LVP may continue to increase induced pulsatility of continuous-flow devices.

Acknowledgment

The authors would like to thank Dr. Eric Pardyjak at the University of Utah for his assistance. This work was funded in part by the National Institutes of Health R01HL089592 (CHS).

References

[1] Wesolowski, S. A., Fisher, J. H., and Welsh, C. S., 1953, "Perfusion of the Pulmonary Circulation by Nonpulsatile Flow," Surgery, **33**(3), pp. 370–375.

[2] Nose, Y., 1992, "Is a Pulsatile Cardiac Prosthesis a Dying Dinosaur?" Artif. Organs, **16**(3), pp. 233–234.

[3] Hindman, B. J., Dexter, F., Ryu, K. H., Smith, T., and Cutkomp, J., 1994, "Pulsatile versus Nonpulsatile Cardiopulmonary Bypass: No Difference in Brain Blood Flow or Metabolism at 27 °C," Anesthesiology, **80**(5), pp. 1137–1147, Available at: http://journals.lww.com/anesthesiology/Abstract/1994/05000/Pulsatile_Versus_Nonpulsatile_Cardiopulmonary.23.aspx

[4] Pagani, F. D., Miller, L. W., Russell, S. D., Aaronson, K. D., John, R., Boyle, A. J., Conte, J. V., Bogaev, R. C., MacGillivray, T. E., Naka, Y., Mancini, D., Massey, H. T., Chen, L., Klodell, C. T., Aranda, J. M., Moazami, N., Ewald, G. A., Farrar, D. J., and Frazier, O. H., 2009, "Extended Mechanical Circulatory Support With a Continuous-Flow Rotary LVAD," J. Am. Coll. Cardiol., **54**(4), pp. 312–321.

[5] Slaughter, M. S., Rogers, J. G., Milano, C. A., Russell, S. D., Conte, J. V., Feldman, D., Sun, B., Tatooles, A. J., Delgado, R. M., Long, J. W., Wozniak, T. C., Ghumman, W., Farrar, D. J., and Frazier, O. H., 2009, "Advanced Heart Failure Treated With Continuous-Flow LVAD," New Engl. J. Med., **361**, pp. 2241–2251.

[6] Nose, Y., 1988, "The Need for a Nonpulsatile Pumping System," Artif. Organs, **12**(2), pp. 113–115.

[7] Unger, F., 1986, "Review Article: Current Status and Use of Artificial Hearts and Circulatory Assist Devices," Perfusion, **1**(3), pp. 155–163.

[8] Olsen, D. B., 2000, "The History of Continuous-Flow Blood Pumps," Artif. Organs, **24**(6), pp. 401–404.

[9] Allen, G. S., Murray, K. D., and Olsen, D. B., 1997, "The Importance of Pulsatile and Nonpulsatile Flow in the Design of Blood Pumps," Artif. Organs, **21**(8), pp. 922–928.

[10] Potapov, E. V., Loebe, M., Nasseri, B. A., Sinawski, H., Koster, A., Kuppe, H., Noon, G. P., DeBakey, M. E., and Hetzer, R., 2000, "Pulsatile Flow in Patients With a Novel Nonpulsatile Implantable VAD," Circulation, **102**(19 Suppl. 3), pp. III183–III187.

[11] Griffith, B. P., Kormos, R. L., Borovetz, H. S., Litwak, K., Antaki, J. F., Poirier, V. L., and Butler, K. C., 2001, "HeartMate II LVAS: From Concept to First Clinical Use," Ann. Thorac. Surg., **71**(3 Suppl.), pp. S116–S120.

[12] Choi, S., Antaki, J. F., Boston, J. R., and Thomas, D. A., 2001, "Sensorless Approach to Control of a Turbodynamic LVAS," IEEE T. Contr. Syst. T., **9**(3), pp. 473–482.

[13] Pantalos, G. M., Koenig, S. C., Gillars, K. J., Giridharan, G. A., and Ewert, D. L., 2004, "Characterization of an Adult Mock Circulation for Testing Cardiac Support Devices," ASAIO J., **50**(1), pp. 37–46.

[14] Stanfield, J. R., Selzman, C. H., Pardyjak, E. R., and Bamberg, S. M., 2012, "Flow Characteristics of Continuous-Flow LVADs in a Novel Open-Loop System," ASAIO J., **58**(6), pp. 590–596.

[15] Stanfield, J. R., and Selzman, C. H., 2012, "Pressure Sensitivity of Axial-Flow and Centrifugal-Flow LVADs," Cardiovasc. Eng. Tech., **3**(4), pp. 413–423.

[16] Choi, S., Boston, J. R., and Antaki, J. F., 2005, "An Investigation of the Pump Operating Characteristics as a Novel Control Index for LVAD Control," Int. J. Cont. Autom., **3**(1), pp. 100–108, Available at: http://bme2.aut.ac.ir/~towhidkhah/BioModelling/Seminar87-1/rohani/An%20investigation%20of%20the%20pump%20operating%20characteristics%20as%20a%20novel%20control%20index%20for%20LVAD%20control.pdf

[17] Choi, S., Boston, J. R., and Antaki, J. F., 2007, "Hemodynamic Controller for LVAD Based on Pulsatility Ratio," Artif. Organs, **31**(2), pp. 114–125.

[18] Stepanoff, A. J., 2011, *Centrifugal and Axial Flow Pumps*, 2nd ed., John Wiley & Sons, New York.

[19] Garcia, S., Kandar, F., Boyle, A., Colvin-Adams, M., Lliao, K., Joyce, L., and John, R., 2008, "Effects of Pulsatile- and Continuous-Flow LVADs on Left Ventricular Unloading," J. Heart Lung Transpl., **27**(3), pp. 261–267.

[20] Klotz, S., Deng, M. C., Stypmann, J., Roetker, J., Wilhelm, M. J., Hammel, D., Scheld, H., H., and Schmid, C., 2004, "Left Ventricular Pressure and Volume Unloading During Pulsatile versus Nonpulsatile LVAD Support," Ann. Thorac. Surg., **77**(1), pp. 143–150.

[21] Haft, J., Armstrong, W., Dyke, D. B., Aaronson, K. D., Koelling, T. M., Farrar, D. J., and Pagani, F. D., 2007, "Hemodynamic and Exercise Performance With Pulsatile and Continuous-Flow LVADs," Circulation, **116**(11 Suppl.), pp. I8–I15.

[22] DiGiorgi, P. L., Smith, D. L., Naka, Y., and Oz, M. C., 2004, "*In Vitro* Characterization of Aortic Retrograde and Antegrade Flow From Pulsatile and Nonpulsatile VADs," J. Heart Lung Transpl., **23**(2), pp. 186–192.

[23] Nakata, K., Shiono, M., Orime, Y., Hata, M., Sezai, A., Saitoh, T., and Sezai, Y., 1996, "Effect of Pulsatile and Nonpulsatile Assist on Heart and Kidney Microcirculation With Cardiogenic Shock," Artif. Organs, **20**(6), pp. 681–684.

[24] Amir, O., Radovancevic, B., Delgado, R. M., Kar, B., Radovancevic, R., Henderson, M., Cohn, W. E., and Smart, F. W., 2006, "Peripheral Vascular Reactivity in Patients With Pulsatile vs. Axial Flow LVAD Support," J. Heart Lung Transpl., **25**(4), pp. 391–394.

[25] Young, J. B., 2001, "Healing the Heart With VAD Therapy: Mechanisms of Cardiac Recovery." Ann. Thorac. Surg., **71**(3 Suppl.), pp. S210–S219.

[26] Levin, H., Oz, M., Chen, J., Packer, M., Rose, E., and Burkhoff, D., 1995, "Reversal of Chronic Ventricular Dilatation in Patients With End-Stage Cardiomyopathy by Prolonged Mechanical Unloading," Circulation, **91**(11), pp. 2717–2720.

[27] Farrar, D. J., Bourque, K., Dague, C. P., Cotter, C. J., and Poirier, V. L., 2007, "Design Features, Developmental Status and Experimental Results With the Heartmate III Centrifugal LVAS With Magnetically Levitated Rotor," ASAIO J., **53**(3), pp. 310–315.